Frequency locking and nonlocal transport in charge-density-wave conductors

S. G. Lemay and R. E. Thorne
Laboratory of Atomic and Solid State Physics, Clark Hall, Cornell University, Ithaca, New York 14853-2501

M. C. Saint-Lager* and P. Monceau
Centre de Recherches sur les Très Basses Températures, Centre National de la Recherche Scientifique, Boîte Postale 166X, 38042 Grenoble Cédex, France

(Received 4 June 1996)

The boundary conditions imposed by current injection electrodes on steady-state sliding of a charge-density wave (CDW) cause the formation of a macroscopic CDW strain field. When two segments of a crystal are independently biased, the resulting strain field can couple CDW transport in these segments. Using a one-dimensional classical deformable medium model that includes phase slip, we calculate how the CDW current in each segment varies with the two biases. The results are in excellent qualitative agreement with experiments on nonlocal CDW behavior in $NbSe_3$, and indicate that the boundary conditions imposed by phase slip and the resulting long-range elastic interactions profoundly affect measured CDW transport properties in experiments utilizing multiple current injection electrodes. [S0163-1829(96)02748-8]

A charge-density wave (CDW) consists of a modulation of the conduction electron density $\delta n(x,t)=n_1\cos[Qx+\theta(x,t)]$ and an associated modulation of the positions of the lattice atoms.[1] Applied electric fields greater than a bulk impurity pinning field E_P cause the CDW to slide with respect to the lattice. In a two-electrode configuration, steady-state sliding is only possible if CDW phase fronts are added near one electrode and removed near the other.[2] This phase slip requires the formation of a macroscopic CDW strain field $\epsilon(x)\equiv(1/Q)(\partial\theta/\partial x)$, the CDW being compressed ($\epsilon>0$) in regions where phase fronts are removed and stretched ($\epsilon<0$) in regions where they are added.[2–5] CDW deformations are not confined to the region between the two electrodes, but penetrate on the order of 100 μm beyond the electrodes in a manner analogous to the Bean critical state of vortices in type-II superconductors.[6]

Long-range interactions arising from these strain fields were probed experimentally by Gill[7] and, more recently, by Saint-Lager and co-workers.[8] The latter investigation found that current injected in a segment of a $NbSe_3$ whisker affects the CDW transport properties of an adjacent segment of the crystal. As shown in the inset to Fig. 1, the experiment employed four electrodes—labeled 1 through 4—separated by distances $l_{mn}=x_m-x_n$. The coherent oscillation frequency ν, which is proportional to the CDW current density, was measured in segments 12 and 34 as a function of the injected currents i_t^{12} and i_t^{34}. The results for i_t^{12} and i_t^{34} both positive are shown in Fig. 1. The two segments are clearly interacting: varying the injected current in one segment affects CDW transport in the other. Particularly striking is the ''locked'' regime, a range of applied currents for which $\nu^{12}=\nu^{34}$. Interactions between transport in the two segments were observed for segment separations l_{32} as large as 100 μm. In contrast, no interactions were observed when i_t^{12} and i_t^{34} had different signs.

Here we show that these experimental results are explained by a one-dimensional (1D) classical deformable medium model where the boundary conditions associated with phase slip are enforced. When i_t^{12} and i_t^{34} are both positive and sufficient to depin the CDW, the addition of the CDW phase at electrode 2 requires the formation of a region of negative CDW strain about that electrode, while the removal of phase at electrode 3 requires the formation of a region of positive strain. If the distance l_{32} is sufficiently small, these strained regions of opposite sign overlap, causing the strain and phase slip rate to be reduced near contacts 2 and 3. When i_t^{12} and i_t^{34} are nearly equal, the strain near electrodes 2 and 3 is small and no phase slip occurs there. Phase fronts

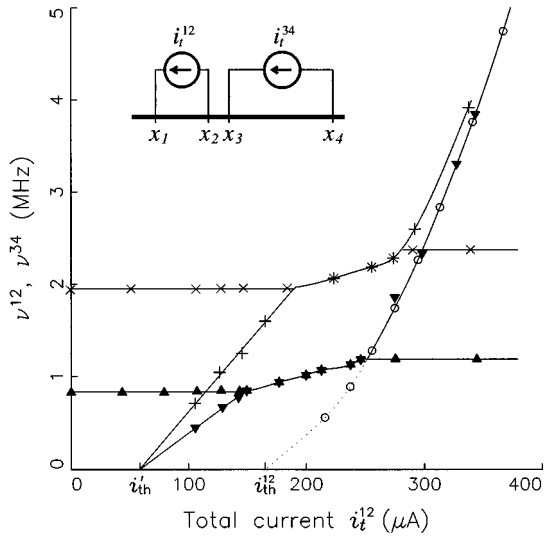

FIG. 1. Measured coherent oscillation frequencies vs applied current i_t^{12} for $i_t^{34}=0$ (ν^{12}:○), $i_t^{34}=100$ μA (ν^{12}: ▼, ν^{34}: ▲), and $i_t^{34}=132$ μA (ν^{12}: +, ν^{34}: ×). Symbols are summarized in the inset to Fig. 2. The solid lines are guides to the eye. The inset shows the experimental geometry; data are from $NbSe_3$ at $T=42$ K with $l_{21}=x_2-x_1=50$ μm, $l_{32}=0$, and $l_{43}=500$ μm. From Ref. 8.

are then generated at electrode 4 only and destroyed at electrode 1 only; the CDW current is uniform between electrodes 1 and 4, and $\nu^{12}=\nu^{34}$. When i_t^{12} and i_t^{34} have opposite signs, the strained regions near contacts 2 and 3 have the same sign and no such cancellation occurs. Phase slip in the two segments is then effectively decoupled and no interaction is observed.

We use the model of Adelman *et al.*,[9] which reproduces the experimental spatiotemporal response of $NbSe_3$'s $T_{P_1}=145$ K CDW to bipolar current pulses. The model treats the CDW as a 1D classical deformable medium. Impurity pinning is modeled by an experimentally determined pinning force $E_P(i_c)$, while phase slip processes are modeled by a local rate of CDW phase generation $r_{\rm ps}(x,t)$ taken to be a function of the local CDW strain $\epsilon(x)$. The equation of motion for θ is

$$\frac{\partial\theta(x,t)}{\partial t}=\left(\frac{Q}{en_cA}\right)i_c(x,t)+\int_{-\infty}^{x}r_{\rm ps}[\epsilon(x',t)]dx', \quad (1)$$

where the CDW current i_c is

$$i_c(x,t)=\frac{1}{\rho_s+\rho_c}\left[\rho_s i_t(x,t)-E_P(i_c)+\kappa\frac{\partial\epsilon(x,t)}{\partial x}\right], \quad (2)$$

and i_t is the total current, ρ_s is the single-particle resistance per unit length, ρ_c is the high-field CDW resistance per unit length, A is the sample cross-sectional area, n_c is the CDW carrier concentration, e is the electronic charge, and $\kappa\equiv(Q^2/en_c)K$ with K the CDW spring constant. The boundary conditions for a steady-state solution ($\partial\theta/\partial t=0$) are the continuity of $\epsilon(x)$ at the electrodes and $i_c\to 0$ for $x\to\pm\infty$.[10]

The above equations are in terms of the macroscopic CDW phase θ as defined by Adelman *et al.*[9] That is, the phase is evaluated at fixed t with respect to a position far from the region where the CDW is sliding. To emphasize the difference between this and earlier conventions, we label the CDW phase by θ instead of the usual ϕ. The two representations are related by

$$\phi(x,t)=\theta(x,t)-\int_{-\infty}^{t}\int_{-\infty}^{x}r_{\rm ps}[\epsilon(x',t')]dx'dt', \quad (3)$$

hence θ and ϕ are interchangeable provided that the strain-slip relation is known. Qualitatively, $\theta(x,t_0)$ describes CDW deformations while $\phi(x_0,t)$ describes CDW sliding. This is illustrated by the condition for steady-state CDW sliding, $\partial\theta/\partial t=0$, which contrasts with the well-known relation $i_c\propto\partial\phi/\partial t$. It is more convenient to use θ here since the elastic strain is given by $(1/Q)(\partial\theta/\partial x)$ even in the presence of phase slip.

To gain insight into the underlying physics, we obtain an approximate analytic solution to Eq. (1). We approximate the pinning force by a constant, $E_P(i_c)=\mathrm{sgn}(i_c)E_P^0$ and the phase slip rate $r_{\rm ps}$ by

$$r_{\rm ps}[\epsilon(x)]=\lim_{\alpha\to\infty}\begin{cases}-\alpha[\epsilon(x)-\epsilon_c], & \epsilon(x)\geq\epsilon_c\\ 0, & |\epsilon(x)|<\epsilon_c\\ \alpha[|\epsilon(x)|-\epsilon_c], & \epsilon(x)\leq-\epsilon_c.\end{cases} \quad (4)$$

No phase slip occurs for strain less than a critical value ϵ_c; beyond ϵ_c, an arbitrarily small increase in strain results in an arbitrarily large slip rate. This mimics the sharp turn-on of $r_{\rm ps}$ predicted by Ramakrishna *et al.*[11] for bulk nucleation,

$$r_{\rm ps}[\epsilon(x)]=-\mathrm{sgn}[\epsilon(x)]r_0\exp\left[-\frac{V_a}{2\kappa|\epsilon(x)|}\right], \quad (5)$$

in which the parameters r_0 and V_a are determined experimentally.[9] With these approximations, all phase slip occurs at the current injection electrodes. Equations (1) and (2) reduce in the steady state to first-order polynomials in $\epsilon(x_1)$, $\epsilon(x_2)$, $\epsilon(x_3)$, $\epsilon(x_4)$, i_c^{12}, and i_c^{34} with only three independent parameters: E_P^0/ρ_s, $\kappa\epsilon_c/\rho_s$, and ρ_c/ρ_s.

We first relate $\kappa\epsilon_c$ to a measurable quantity. When the total current is i_t^{mn} in segment mn and zero everywhere else, Eq. (1) gives for the CDW current in segment mn

$$|i_c^{mn}|=\begin{cases}(1+\rho_c/\rho_s)^{-1}(|i_t^{mn}|-i_{\rm th}^{mn}), & |i_t^{mn}|\geq i_{\rm th}^{mn}\\ 0 \quad \text{otherwise},\end{cases} \quad (6)$$

where

$$i_{\rm th}^{mn}\equiv[E_P^0+2\kappa\epsilon_c/l_{mn}]/\rho_s. \quad (7)$$

Experimentally, the threshold field for the onset of steady-state CDW conduction is the sum of a bulk term and a boundary-condition-related term: $E_{\rm th}^{mn}=E_P^0+V_{\rm ps}^0/l_{mn}$, where $V_{\rm ps}^0$ is approximately independent of l_{mn}. By Eq. (7), $2\kappa\epsilon_c$ corresponds to the measurable quantity $V_{\rm ps}^0$.

We now give the solution to Eq. (1) when $i_t^{12}\neq 0$ and $i_t^{34}\geq 0$. When i_t^{12} is negative or small, the CDW currents i_c^{12} and i_c^{34} are given by Eq. (6), that is, no coupling between the two segments is apparent. When i_t^{12} exceeds a new effective threshold current $i_{\rm th}'$ the CDW current in segment 12 is

$$\left(1+\frac{\rho_c}{\rho_s}\right)i_c^{12}=\begin{cases}i_t^{12}\dfrac{l_{21}}{l_{31}}-\dfrac{E_P^0}{\rho_s}, & i_{\rm th}'\leq i_t^{12}<i_{\rm lock}^-\\ i_t^{12}\dfrac{l_{21}}{l_{41}}+i_t^{34}\dfrac{l_{43}}{l_{41}}-i_{\rm th}^{41}, & i_{\rm lock}^-\leq i_t^{12}<i_{\rm lock}^+\\ i_t^{12}-i_{\rm th}^{12}, & i_{\rm lock}^+\leq i_t^{12}\end{cases} \quad (8)$$

and that in segment 34 is

$$\left(1+\frac{\rho_c}{\rho_s}\right)i_c^{34}=\begin{cases}i_t^{34}\dfrac{l_{43}}{l_{41}}+i_t^{12}\dfrac{l_{21}}{l_{41}}-i_{\rm th}^{41}, & i_{\rm lock}^-\leq i_t^{12}\leq i_{\rm lock}^+\\ i_t^{34}\dfrac{l_{43}}{l_{42}}-\dfrac{E_P^0}{\rho_s}, & i_{\rm lock}^+\leq i_t^{12},\end{cases} \quad (9)$$

where we have defined

$$i_{\rm th}'=(E_P^0/\rho_s)(l_{31}/l_{21}), \quad (10)$$

$$i_{\rm lock}^-=i_{\rm th}'+(l_{31}/l_{21})(i_t^{34}-i_{\rm th}^{34}), \quad (11)$$

$$i_{\rm lock}^+=i_t^{34}(l_{43}/l_{42})+2\kappa\epsilon_c/(\rho_s l_{21}). \quad (12)$$

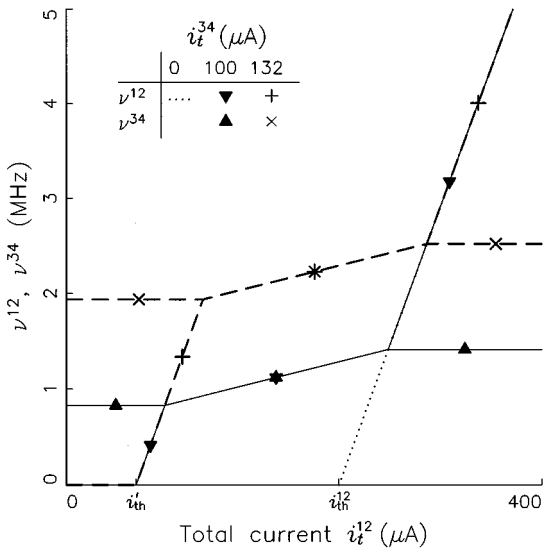

FIG. 2. Approximate analytical result of Eqs. (8) and (9) for the coherent oscillation frequencies ν^{12} and ν^{34} vs current i_t^{12} for three values of i_t^{34}. Material parameters and electrode geometry are as per the experiment of Fig. 1.

The currents $i_{\rm lock}^-$ and $i_{\rm lock}^+$ delimit a locking regime where $i_c^{12}=i_c^{34}$ This solution is valid provided that l_{32} and $i_{\rm th}^{34}$ are sufficiently small.[12]

The coherent oscillation frequencies $\nu=(Q/2\pi en_cA)i_c$ predicted by Eqs. (8) and (9) are plotted in Fig. 2.[13] Typical strain profiles $\epsilon(x)$ for selected values of i_t^{12} are plotted in Fig. 3.

Equations (8) and (9) compare favorably with experiment. Saint-Lager and co-workers[8] found that $i'_{\rm th}=E_P^0/\rho_s$ when $l_{32}\rightarrow 0$. This is the relationship predicted by Eq. (10). They also found that frequency locking occurs for currents in the range $i_t^{12}\simeq i_t^{34}$ to $i_t^{12}\simeq i_t^{34}+V_{\rm ps}^0/\rho_s l_{21}$, again for $l_{32}\rightarrow 0$. The upper bound agrees with Eq. (12) for $i_{\rm lock}^+$. The lower bound differs from Eq. (11) for $i_{\rm lock}^-$ by $V_{\rm ps}^0/\rho_s l_{43}$, but, because l_{43} was large, this quantity is smaller than the experimental accuracy. The good agreement between measured and calculated quantities gives us confidence that the analytical model includes the key interactions involved in the experiment.

This solution yields the following interpretation. For $i_t^{34}>i_{\rm th}^{34}$ and $i_t^{12}=0$, there are strained regions beyond contacts 3 and 4 that support the strain necessary for phase slip to occur at those contacts, as shown in Fig. 3(a). The spatial extent of these regions is dictated by the maximum strain gradient that can be supported by impurity pinning, $\partial\epsilon/\partial x|_{\rm max}=E_P^0/\kappa$, and for $l_{32}<\kappa\epsilon_c/E_P^0$ the strained region beyond contact 3 extends into segment 12. As i_t^{12} is increased from zero, the strain gradient in segment 12 is reduced and the strained region extends further to the left [Fig. 3(b)]. If i_t^{12} is increased beyond $i'_{\rm th}$ the strain at x_1 reaches ϵ_c, phase slip starts occurring at contact 1, and the CDW slides in both segments 12 and 23 [Fig. 3(c)]. In this regime, the CDW current in segment 12 is due to CDW phase fronts generated at contact 4; no phase slip occurs at contact 2. If i_t^{12} is increased beyond $i_{\rm lock}^-$ the strain $\epsilon(x_3)$ is relieved. As shown in Fig. 3(d), we then have $|\epsilon(x_2)|,|\epsilon(x_3)|<\epsilon_c$ and no phase slip occurs at electrodes 2 and 3. This implies that

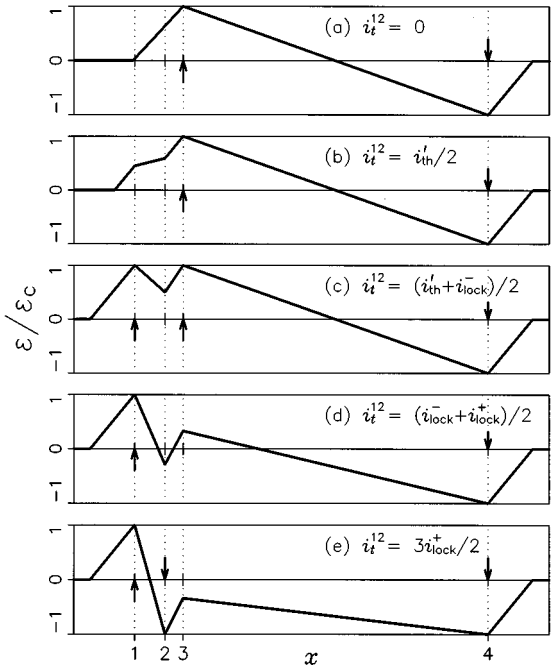

FIG. 3. Analytical result for the strain profiles $\epsilon(x)$ for $i_t^{34}=4i_{\rm th}^{34}/3$ and selected values of i_t^{12}. The arrows indicate contacts where phase slip is occurring. For (a) $i_t^{12}=0$, the strain associated with conduction in segment 34 extends beyond electrodes 3 and 4. For (b) $0<i_t^{12}<i'_{\rm th}$ and (c) $i'_{\rm th}<i_t^{12}<i_{\rm lock}^-$ the strain extends further to the left. For (d) $i_{\rm lock}^-<i_t^{12}<i_{\rm lock}^+$ the interaction between segments 12 and 34 results in $|\epsilon(x_2)|,|\epsilon(x_3)|<\epsilon_c$ and no phase slip occurs at electrodes 2 and 3. The CDW current is uniform between electrodes 1 and 4, and ν^{12} and ν^{34} are ''locked.'' For (e) $i_t^{12}>i_{\rm lock}^+$ phase slips occurs at electrode 2 and no locking is observed. The material parameters used are as per the experiment of Fig. 1, but we use $l_{21}=100$ μm, $l_{32}=50$ μm, and $l_{43}=500$ μm to illustrate the general case treated in the text.

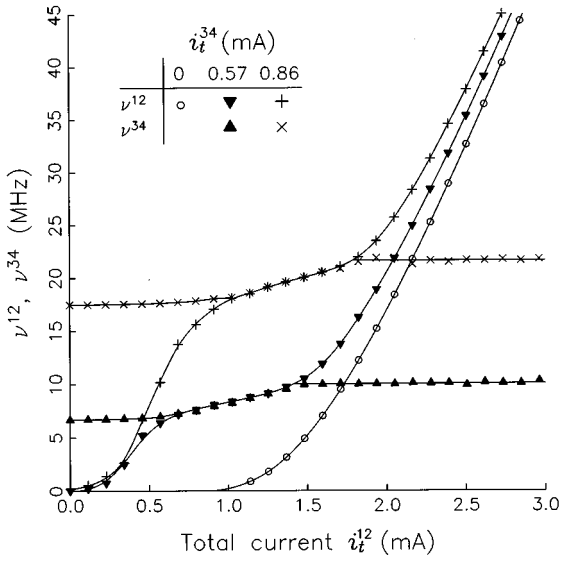

FIG. 4. Computed ν^{12} and ν^{34} vs current i_t^{12} for $i_t^{34}=0$, $i_t^{34}=4i_{\rm th}^{34}/3$ and $i_t^{34}=2i_{\rm th}^{34}$ Electrode geometry is as per the experiment of Fig. 1, but material parameters for $NbSe_3$ at $T=90$ K were used since $T=42$ K values were unavailable.

$i_c^{12}=i_c^{23}=i_c^{34}$ ($\nu^{12}=\nu^{23}=\nu^{34}$) and the sample is in the locked regime. Consequently, the ''frequency locking'' is not an interference phenomenon: it is the result of having uniform CDW sliding from contact 4 to contact 1. If i_t^{12} is increased yet further the strain $\epsilon(x_2)$ becomes more negative until at $i_t^{12}=i_{\rm lock}^{+}$ phase slip starts occurring at contact 2 [Fig. 3(e)], and ν^{12} and ν^{34} differ again. ν^{34} is now greater than when $i_t^{12}=0$ since a smaller strain gradient must be opposed by the applied field in segment 34.

The predictions of the approximate analytic solution can be confirmed by numerically solving Eq. (1) using Eq. (5) for $r_{\rm ps}$ and an experimentally determined $E_P(i_c)$. A quantitative comparison with the experimental data of Fig. 1 was not possible since the required material parameters, in particular the phase slip parameters r_0 and V_a, are not well known for $NbSe_3$ at $T=42$ K. We instead used the $T=90$ K material parameters of Adelman *et al.*[9]

The calculated coherent oscillation frequencies[14] are shown in Fig. 4. Using realistic functions for $r_{\rm ps}(\epsilon)$ and $E_P(i_c)$ improves qualitative agreement with the experiment. Computed strain profiles $\epsilon(x)$ (not shown) exhibit the same behavior as those obtained from the analytic model (Fig. 3), except for phase-slip-induced nonlinearities near the current injection electrodes as discussed by Adelman *et al.*[9]

We emphasize that the phase-slip boundary conditions cannot be ignored in the interpretation of CDW transport experiments involving three or more current injection electrodes. For example, the transient responses measured by Arbaoui and Dumas[15] in the blue bronzes and by Gill[16] in $NbSe_3$ no doubt include a contribution from the establishment of strain fields such as those of Fig. 3.

Finally, we note that this interpretation makes a further prediction. In the locked regime and for $l_{32}>0$ there is a finite CDW current $i_c^{23}=i_c^{12}=i_c^{34}$ in segment 23. The total current in segment 23 is zero, however, so that a normal current $i_n^{23}=-i_c^{23}$ is also present. A voltage $V^{32}=-i_c^{23}\rho_s l_{32}$ is therefore predicted to appear in the locked regime. This effect provides a way of decoupling the CDW and single-particle conduction channels without applying temperature gradients.[17]

We wish to acknowledge fruitful discussions with T. L. Adelman and M. C. de Lind van Wijngaarden. This work was supported by NSF Grants No. INT-9016655 and No. DMR94-24572. S.G.L. acknowledges support from NSERC.

*Permanent address: Laboratoire de Cristallographie, CNRS, BP 166, 38042 Grenoble Cédex 9, France.

[1] For comprehensive reviews of CDW's, see P. Monceau, *Electronic Properties of Quasi-One-Dimensional Materials* (Reidel, Dordrecht, 1985), Pt. II, p. 139; G. Grüner, Rev. Mod. Phys. **60**, 1129 (1988).

[2] For a review of previous work on CDW phase slip, see J. C. Gill, in *Physics and Chemistry of Low-Dimensional Inorganic Conductors*, edited by C. Schlenker and M. Greenblatt (Plenum, New York, 1996).

[3] L. Mihály and A. Janossy, Phys. Rev. B **30**, 3530 (1984); S. E. Brown, L. Mihály, and G. Grüner, Solid State Commun. **58**, 231 (1986).

[4] D. DiCarlo, E. Sweetland, M. Sutton, J. D. Brock, and R. E. Thorne, Phys. Rev. Lett. **70**, 845 (1993).

[5] M. E. Itkis and J. W. Brill, Phys. Rev. Lett. **72**, 2049 (1994); M. E. Itkis, B. M. Emerling, and J. W. Brill, Phys. Rev. B **52**, R11 545 (1995).

[6] M. Tinkham, *Introduction to Superconductivity* (McGraw-Hill, New York, 1975), p. 173.

[7] J. C. Gill, Solid State Commun. **44**, 1041 (1982).

[8] M. C. Saint-Lager, P. Monceau, and M. Renard, Europhys. Lett. **9**, 585 (1989); Synth. Met. **29**, F279 (1989); M. C. Saint-Lager, Ph.D. thesis, Université de Grenoble, 1988.

[9] T. L. Adelman, M. C. de Lind van Wijngaarden, S. V. Zaitsev-Zotov, D. DiCarlo, and R. E. Thorne, Phys. Rev. B **53**, 1833 (1996).

[10] It is also assumed when plotting $\epsilon(x)$ that i_t^{12} and i_t^{34} are increased monotonically from zero so as to uniquely specify the strain outside the outermost electrodes. This is irrelevant to the calculation of i_c.

[11] S. Ramakrishna, M. P. Maher, V. Ambegaokar, and U. Eckern, Phys. Rev. Lett. **68**, 2066 (1992).

[12] The solution of Eqs. (8) and (9) is valid when (1) $i_c^{34}>i_{\rm th}^{34}$ where we chose i_t^{34} positive for definiteness, (2) $l_{32}<2\kappa\epsilon_c/E_P^0$ (segments 12 and 34 decouple for larger l_{32}), and (3) $i_t^{34}<(2\kappa\epsilon_c/\rho_s)(l_{42}/l_{43}l_{32})$ (the locking regime vanishes for larger i_t^{34}). The values of the parameters extracted from the experimental data of Fig. 1 satisfy these conditions.

[13] Figures 2 and 3 use $E_P^0/\rho_s=59$ μA, $\kappa\epsilon_c/\rho_s=4300$ μm μA and $(Q/2\pi e n_c A)(1+\rho_c/\rho_s)^{-1}=0.034$ MHz/μA. These values were determined from the experimental values of $i_{\rm th}'$ $i_{\rm th}^{12}$ and $d\nu^{12}/di_t^{12}$ at high i_t^{12} respectively.

[14] To mimic how ν is determined from experimental spectra, the calculated frequency was determined from the peak of a histogram of the position-dependent CDW current $i_c(x)$. The discreteness of the histogram causes the slight ripple in Fig. 4.

[15] A. Arbaoui, A. Ayadi, and J. Dumas, Synth. Met. **56**, 2682 (1993).

[16] J. C. Gill, Europhys. Lett. **11**, 175 (1990).

[17] W. P. Beyermann, L. Mihály, and G. Grüner, Phys. Rev. Lett. **56**, 1489 (1986).